

INVESTIGATION OF THE ENHANCED SPATIAL
DENSITY OF SUBMICRON LUNAR EJECTA BETWEEN
L VALUES 1.2 AND 3.0 IN THE EARTH'S MAGNETOSPHERE: THEORY

W.M. Alexander, W.G. Tanner, H.S. Goad
Space Science Laboratory, Department of Physics
Baylor University, Waco, Texas

INTRODUCTION

Initial results from the measurement conducted by the dust particle experiment on the lunar orbiting satellite Lunar Explorer 35 (LE 35) have been reported by Alexander et al. (1,2,3,4) with the data interpreted as indicating that the moon is a significant source of micrometeoroids. Primary sporadic and stream meteoroids impacting the surface of the moon at hypervelocity has been proposed as the source of micron and submicron particles that leave the lunar craters with velocities sufficient to escape the moon's gravitational sphere of influence. No enhanced flux of lunar ejecta with masses greater than a nanogram was detected by LE 35 or the Lunar Orbiters (5). Hypervelocity meteoroid simulation experiments concentrating on ejecta production (6,7,8,9) combined with extensive analyses (10,11,12,13) of the orbital dynamics of micron and submicron lunar ejecta in selenocentric, cislunar and geocentric space have shown that a pulse of these lunar ejecta, with a time correlation related to the position of the moon relative to the earth, intercepts the earth's magnetopause surface (EMPs). As shown by Alexander et al. (14), a strong reason exists for expecting a significant enhancement of submicron dust particles in the region of the magnetosphere between L values of 1.2 and 3.0. This is the basis for the proposal of a series of experiments to investigate the enhancement or even trapping of submicron lunar ejecta in this region. The subsequent interaction of this mass with the upper-lower atmosphere of the earth and possible geophysical effects can then be studied.

FORMATION OF LUNAR EJECTA

An analysis of the data from the dust particle experiment on LE 35 provided the basis for the determination of some of the parameters of lunar ejecta escaping the surface of the moon (1,2,3,4). The primary reason for this interpretation resulted from a significant change in the event rate detected by the experiment during periods associated with the passage of the earth-moon system through the major annual meteor streams. This feature of the data occurred for five consecutive years. The event rate during non-meteor shower periods was essentially the same as the interplanetary rates. An additional fact was no enhancement of the event rate for nanogram size lunar ejecta which is consistent with the measurements reported by Gurtler and Grew (5).

Hypervelocity meteoroid simulation experiments (6,7,8,9) have provided ratios relating the mass of the impacting particle to the mass of ejecta produced. In order to discover the ratio, the effects of particle density as well as impact angle of incidence have been examined. Schneider (7) has found that a 10 mg particle with a velocity of 4 km/s impacting at normal incidence would produce ejecta which represented 7.5×10^{-5} the mass of the incident particle and had a velocity greater than 3 km/s. Alexander (8) has shown that under similar initial conditions the ejecta mass ratio, e , would be higher by an order of magnitude ($e = 5 \times 10^{-4}$). A recent study by Zook et al. (24) reported that oblique angle impacts would produce 200 to 300 times more microcraters (diameters = 7 μm) on ejecta

measuring plates than would be produced by normal incidence impacts. Given that 7 μ m diameter microcraters correspond to particles with $m = 10^{-12}$ g (14) and that the impact velocity was 6.7 km/s, one may infer that the fraction of ejecta mass with lunar escape velocity would also increase by 200 to 300 times ($e = 1.5 \times 10^{-2}$). These three values for the "ejecta to incident particle mass" ratios will be employed to establish the total lunar ejecta mass after the interplanetary flux at 1 AU has been determined (15).

Three recent dust flux models are used for the basic calculations that are reported in this paper. The first was given by McDonnell (16) then updated by McDonnell et al. (17). The second one is that of Grun et al. (18), followed by the flux curve derived from lunar crater data as presented by Morrison and Zinner (19). The Log of cumulative flux versus the Log of particle mass for each model is depicted in Fig. 1 (20). McDonnell (17) model is based on the relevant flux measurements in the vicinity of 1 AU heliocentric distance corrected for Earth shadowing and reduced to a flat surface exposure geometry. The curve in Fig. 1 labeled Grun, reported as Model 1 (18), is a lunar flux model. The first two curves in Fig. 1 are based primarily on in-situ measurements in space and are seen to be quite similar for cumulative masses $> 10^{-12}$ g. The most pronounced similarity which can be observed is the mass distribution index of both curves, which is the slope of the Log-Log depiction of the two cumulative curves. The third model, derived from lunar crater data of Morrison and Zinner (19), is shown as a Log cumulative flux vs. a Log mass distribution. One can observe that for masses $< 10^{-12}$ g the divergence between the three mass models appears to be most drastic. Considerable attention has been given to the variations in the cumulative flux of submicron particles suggested by these models (21). In summary, a bimodal particle distribution may exist near the moon, especially where the in-situ measurements are in selenocentric space.

The next most important step is to use the cumulative flux models to determine the total mass of sporadic interplanetary matter impacting the lunar surface. Hughes (22) has shown that the cumulative flux of particles on a surface (per unit area per unit time) have a mass m is:

$$\Psi = \epsilon(m)m = Am^{1-\alpha} dm. \quad (1)$$

(where A is a constant and α is the mass distribution index). The Log differential mass flux vs. Log mass curves derived from the three mass models depicted in Fig. 1 are shown in Fig. 2 (20); the total mass flux of sporadic meteoroids impacting the lunar surface is determined with the results give in Table I. (The mass range for each model is 10^{-18} - 10^{+2} g. The information contained in Table I provides the initial basis for a model of the ejecta mass.

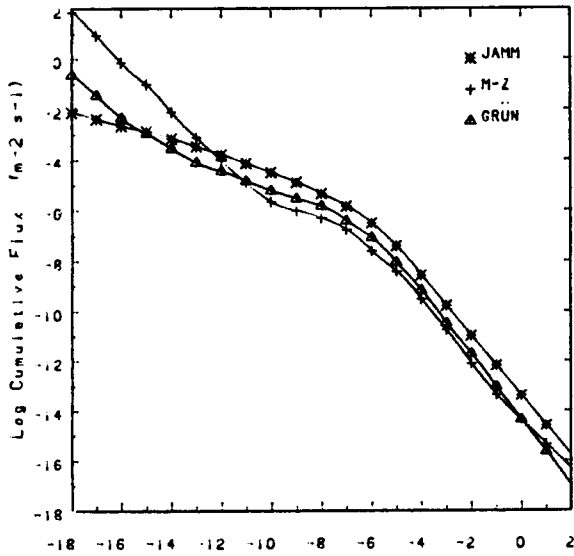


Figure 1. Log Mass (grams)

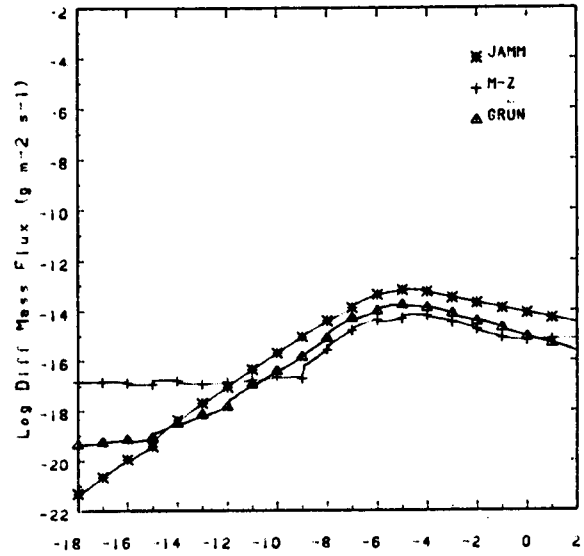


Figure 2. Log Mass (grams)

TABLE I

Model	Mass Flux g/m ² sec	Total Mass Lunar Surface g / Day
McDonnell	2.5×10^{-12}	8.3×10^6
Grun	5.5×10^{-13}	1.8×10^6
Morrison-Zinner	2.4×10^{-13}	8.0×10^5

Production of ejecta during hypervelocity impact events have always been observed, and there exist a few notable examples (23) of experiments which have measured the physical and dynamic properties of the ejecta. However only a few sources (21) have provided information concerning the dynamics of that portion of the ejecta which has sufficient velocity to escape the moon. The morphology of craters resulting from hypervelocity impact of micron and submicron particles provides a means of determining (21):

1. The total mass flux of ejecta as a function of primary particle mass, and
2. The cumulative mass distribution of the high velocity ejecta.

Velocities of the primary particles were near 4 km/sec. Zook et al. (24) have recently reported results of similar ejecta studies with an impacting velocity of 6.7 km/sec, but with primary incident angle varying between 7 and 90 degrees.

The major difference between the early results and those of Zook is in the amount of total micron size ejecta mass. Zook has found an increase of a factor of two hundred in the number of one-micron ejecta craters per impacting mass at the oblique angles. An additional ejecta parameter that is common to the studies (25,26,24) is an estimate of the cumulative size distribution for the high velocity micron size ejecta from which the important parameter α , the mass distribution index, can be determined. Such an index can be inferred from the information Schneider reported (21). Table II gives the value of α for each reported instance.

TABLE II
MASS DISTRIBUTION INDEX

Richards (25)	0.81
Alexander & Corbin (26)	0.83
Zook et al. (24)	0.81

TABLE III

SOURCE	TOTAL EJECTA MASS FLUX (g/m ² sec)
Ref. (25) and McDonnell Model	1.24 x 10 ⁻¹⁵
Ref. (26) and McDonnell Model	same results as above
Ref. (24) and McDonnell Model	2.5 x 10 ⁻¹³

Given the total ejecta mass of interest and the mass distribution index, the cumulative flux for the ejecta leaving the moon's sphere of influence can be estimated. This flux can be compared over the ejecta mass range to that of the sporadic micron cumulative flux. Finally, the ejecta spatial density near the lunar surface is given for comparison to that of interplanetary dust flux in Table I. Using the mass flux of Table III and ejecta velocity near the lunar surface of 3 km/sec, Ref. (24) and McDonnell, the spatial densities of the two results in Table III are 4 x 10⁻¹⁹ g/m³, Ref. (25,26), and 8 x 10⁻¹⁷ g/m³, Ref. (24). The above results show that the lunar ejecta spatial density (25,26) near the lunar surface is essentially the same as the incoming interplanetary dust spatial density of 3.2 x 10⁻¹⁹ g/m over the same range of mass. In the second case (24), the ejecta spatial density is greater than that of the interplanetary dust over the same range of mass.

TRANSPORT OF LUNAR EJECTA TO THE MAGNETOSPHERE OF THE EARTH

Alexander et al. (14) have presented the results of a study of the dynamics of micron and submicron particles in selenocentric, cislunar and geocentric space which

shows a significant variation in time of the magnitude of lunar ejecta arriving at the boundary of the magnetosphere. In addition, Corbin (27) determined that the transport time of these particles to the magnetosphere surface varied in such a manner as to effectively focus the particles due to this temporal variation. For example, $0.3 \mu\text{m}$ particles that leave the lunar surface when the LPA is about 105° will arrive at the earth's magnetosphere (EMP_s) within 7 days. A $0.05 \mu\text{m}$ particle released when the LPA is about 155° has a transport time to the EMP_s of less than 2 days (27). Thus, a lunar ejecta flux (LEF_x) of 0.3 and $0.05 \mu\text{m}$ particles will arrive at the surface of the EMP_s essentially at the same time. Shown in Fig. 3 (14) is a LPA and part of a lunar orbit where a large percent of ejecta moves in orbits that will intercept the magnetosphere.

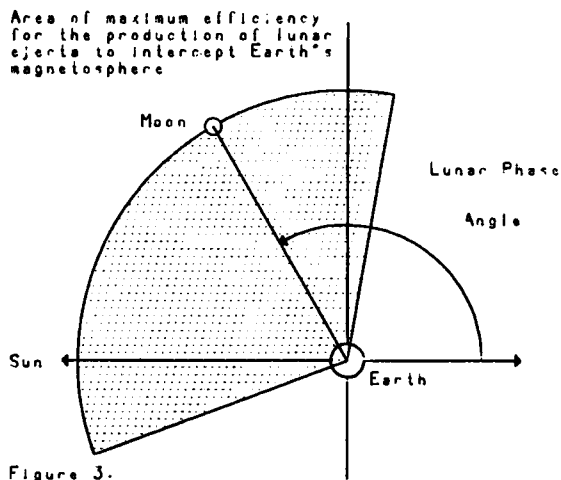


Figure 3.

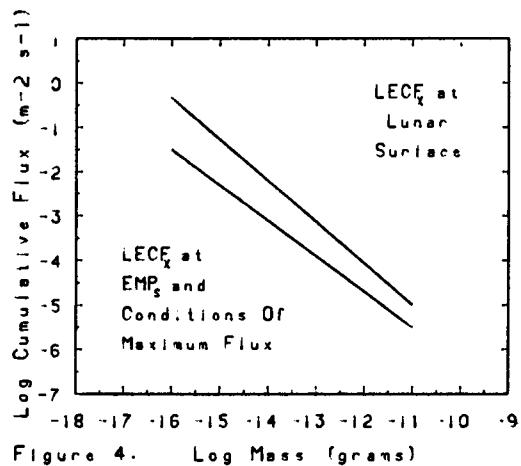


Figure 4.

A sensible qualitative picture combining the percentage ejecta injection from (10) and the transport times from (27) is depicted in Fig. 4 (14). This figure shows a comparison of the lunar ejecta cumulative flux (LECF_x) at the surface of the moon and at the surface of the EMP_s . The flattening of the LECF_x from the position near the lunar surface to the EMP_s surface due to the focusing effect is apparent. This flattening of the LECF_x is the result of the orbit selection as a function of lunar ejecta radius and the non-gravitational forces.

When lunar ejecta arrive at the EMP_s surface, they represent the mass leaving the moon at an LPA of 40° to 170° or about $1/3$ of the time of a lunar orbit. However, the efficient LPA position for lunar ejecta transport with maximum EMP_s interception is between 80° and 160° or over six days of a lunar orbit time, which is approximately $1/4$ of a lunar period. When the lunar ejecta mass is intercepted at the EMP_s boundary, the

LECF_x of micron and submicron particles traverses the EMP_s in a time of slightly more than one day. This represents a focusing effect of at least a factor of three, but not greater than a factor of six. The effect discussed above is depicted in Fig. 5a and 5b (14).

In Fig. 5a (14), the percent of lunar ejecta intercepted by the EMP_s of four different size ejecta particles is shown as a function of LPA or position of the moon when the lunar ejecta was created. Fig. 5b (14) shows the percent of lunar ejecta that is intercepted at the EMP_s surface at essentially the same time. The moon is passing through an LPA of 194° ± 6° during this period.

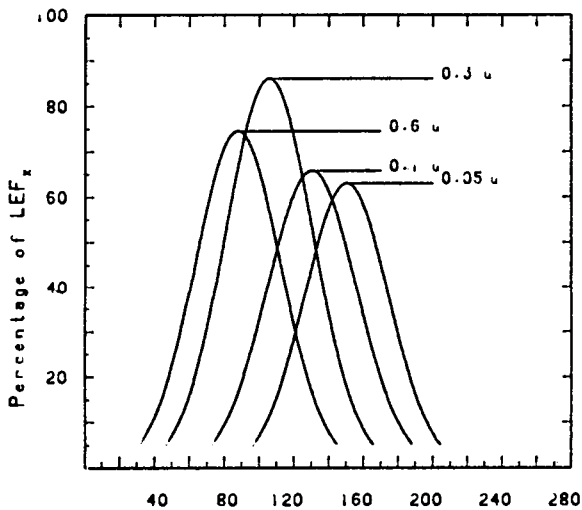


Figure 5a. Lunar Phase Angle

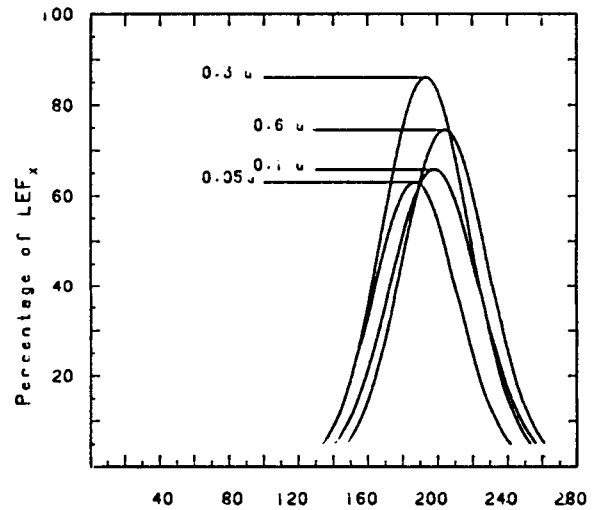


Figure 5b. Lunar Phase Angle

An additional factor of major importance to this work is that of lunar longitude at the time of impact of a primary particle. While the LPA is the major determining lunar position factor, the combination of LPA and longitude produces the maximum LECF_x onto the EMP_s surface. This is demonstrated in Table I where all percentages are calculated for the LPA range (in 10° steps) from 10° to 160° (28).

TABLE I

Lunar Longitude Quarter	Average Percent EMP _s Intercept	Maximum Percent EMP _s Intercept	LPA ^o
1st	20.230	63.89	100
2nd	27.26	77.78	90
3rd	38.28	94.44	110
4th	33.25	90.28	110

The most important factor regarding sensitivity to longitude is the occurrence of non-random impact flux events. This is quite noticeable for the periods known as major shower periods (29). Initially, the LPA will determine if these ejecta will be transported to the EMP_s surface. For an optimal LPA, the maximum LECF_x will occur when the lunar quarter (by longitude definition) is in the most favorable impact position with respect to the meteor shower radiant. From Table I, a shower radiant that was essentially normal to the 3rd and 4th quarter with an LPA near 110^o, would result in greater than 90 percent of the produced ejecta intercepting the EMP_s surface.

CONCLUSIONS

There is ample evidence now to support the concept that the impact of interplanetary dust on the moon's surface creates a significant flux of lunar ejecta which, for nanogram and smaller particles, have lunar escape velocity. When these ejecta are formed during favorable LPAs, i.e. 80^o to 160^o, a large percent of the total mass penetrates the earth's magnetopause as a "pulse" of lunar ejecta. The pulse occurs for each orbit of the moon. The ejecta source is the total mass of interplanetary dust representing the sporadic meteoroids constantly impacting the surface of the moon. When the earth-moon system is intercepting a major meteor stream, the lunar ejecta flux is significantly enhanced if the "meteor shower" time period coincides with an appropriate LPA period (30). An additional enhancement can occur when the lunar "longitude" is also favorable. The possible concentration of these particles in the inner magnetosphere, measurements to study this enhanced spatial density and possible implications to geophysics phenomena is discussed in the following paper by Alexander et al. (31).

REFERENCES

1. W.M. Alexander, C.W. Arthur, J.D. Corbin, and J.L. Bohn, Space Research X, 252 (1970)
2. W.M. Alexander, C.W. Arthur, and J.L. Bohn, Space Research XI, 279 (1971)
3. W.M. Alexander, C.W. Arthur, J.L. Bohn, J.H. Johnson, and B.J. Farmer, Space Research XII, 349 (1972)
4. W.M. Alexander, C.W. Arthur, J.L. Bohn, and J.C. Smith, Space Research XIII, 1037 (1973)
5. C.A. Gurtler and G.W. Grew, Science 161, 462 (1968)
6. D. Gault, NASA TND-1767 (1963)
7. E. Schneider, The Moon 13, 173 (1974)
8. W.M. Alexander, Ph.D. Dissertation, University of Heidelberg, (1975)
9. D.E. Gault, F. Horz and J.B. Hartung, Proc. 3rd Lunar Sci. Conf.: Geochim. Cosmochim. Acta., Suppl. 3 3, 2713 (1972)
10. J. Chanberlain, W.M. Alexander and J. Corbin, IAU Symposium #90 (1979)
11. W.M. Alexander and J. Corbin, IAU Symposium #90 (1979)
12. J. Corbin and W.M. Alexander, Adv. Space Res. Vol. 1, 103 (1981)
13. W.M. Alexander and J. Corbin, Adv. Space Res. Vol. 1, 107 (1981)
14. W.M. Alexander, P. Anz, T. Hyde, A. Hargrave, L. Lodhi, S. Lodhi and W. Tanner, Adv. Space Res. Vol. 4, #9, 27 (1984)
15. W.M. Alexander and W.G. Tanner, SSPEX Workshop, 28 (1985)
16. A. McDonnell, COSMIC DUST, 337, John Wiley and Sons publ. (1978)
17. A. McDonnell, W. Carey and D. Dixon, Nature, #309, 237 (1984)
18. E. Grun, H. Fechtig, H. Zook and R. Reise, Lunar and Planet. Sci. XIV, 267 (1983)
19. D. Morrison and E. Zinner, Proc. Lunar Planet. Sci. Con. 8, 846 (1977)
20. W.M. Alexander, P. Anz, D. Lyons, W. Tanner, Y-L Chen and A. McDonnell, Adv. Space Res. Vol. 4, #9, 23 (1984)
21. E. Schneider, THE MOON 13, 173, (1974)
22. D. Hughes, Spa. Res. XIV, 780 (1974)
23. R. Flavill, R. Allison, A. McDonnell, Proc. Lunar Sci. Conf. 9, 2539 (1978)

24. H. Zook, G. Lange, E. Grun and H. Fechtig, *Lunar and Planet. Sci.* XV, 965 (1984)
25. M. Richards, unpubl. MS Thesis, Baylor University (1975)
26. W.M. Alexander and D. Corbin, *Spa. Res.* XIX, 463 (1979)
27. J. Corbin, unpubl. Ph.D. Dissertation, Baylor University (1980)
28. T. Hyde, unpubl. MS Thesis, Baylor University (1980)
29. W.M. Alexander and W.G. Tanner, *SSPEX Workshop*, 31 (1985)
30. W.M. Alexander and J.D. Corbin, *Adv. Space Res.* 1, 107 (1981)
31. W.M. Alexander, W.G. Tanner and H.S. Goad, this publication, (1986)